Prediction of venous metastases, recurrence, and prognosis in hepatocellular carcinoma based on a unique immune response signature of the liver microenvironment

Anuradha Budhu,[1] Marshonna Forgues,[1] Qing-Hai Ye,[2] Hu-Liang Jia,[1,2] Ping He,[3] Krista A. Zanetti,[4] Udai S. Kammula,[5] Yidong Chen,[6] Lun-Xiu Qin,[2] Zhao-You Tang,[2,*] and Xin Wei Wang[1,*]

[1] Liver Carcinogenesis Section, Laboratory of Human Carcinogenesis, Center for Cancer Research, National Cancer Institute, Bethesda, Maryland 20892
[2] Liver Cancer Institute and Zhongshan Hospital, Fudan University, Shanghai 200032, China
[3] Division of Hematology, Center for Biologics Evaluation and Research, Food and Drug Administration, Bethesda, Maryland 20892
[4] Molecular Genetics and Carcinogenesis Section, Laboratory of Human Carcinogenesis and Cancer Prevention Fellowship Program, Division of Cancer Prevention, National Cancer Institute, Bethesda, Maryland 20892
[5] Surgery Branch, National Cancer Institute, Bethesda, Maryland 20892
[6] Laboratory of Cancer Genetics, National Human Genome Research Institute, Bethesda, Maryland 20892
*Correspondence: xw3u@nih.gov (X.W.W.); zytang8@yahoo.com.cn (Z.-Y.T.)

Summary

Hepatocellular carcinoma (HCC) is an aggressive malignancy mainly due to metastases or postsurgical recurrence. We postulate that metastases are influenced by the liver microenvironment. Here, we show that a unique inflammation/immune response-related signature is associated with noncancerous hepatic tissues from metastatic HCC patients. This signature is principally different from that of the tumor. A global Th1/Th2-like cytokine shift in the venous metastasis-associated liver microenvironment coincides with elevated expression of macrophage colony-stimulating factor (CSF1). Moreover, a refined 17 gene signature was validated as a superior predictor of HCC venous metastases in an independent cohort, when compared to other clinical prognostic parameters. We suggest that a predominant humoral cytokine profile occurs in the metastatic liver milieu and that a shift toward anti-inflammatory/immune-suppressive responses may promote HCC metastases.

Introduction

Cancer metastasis is a complex multistep process that involves alterations in dissemination, invasion, survival, and growth of new cancer cell colonies and the development of cancer-associated vasculature (Hanahan and Weinberg, 2000; Liotta, 1985). Recently, the traditional metastasis paradigm has been challenged by the observations that most of the genetic and epigenetic changes necessary for metastasis appear to be the hallmarks of cancer (Bernards and Weinberg, 2002; Hanahan and Weinberg, 2000). For example, the molecular signature in primary tumors from gene expression profiling studies predict cancer patient metastasis and survival (Ramaswamy et al., 2003; van de Vijver et al., 2002; Ye et al., 2003). Since microarrays detect signals contributed by the bulk of the tissues examined, the results suggest that a majority of primary tumor cells have acquired changes that favor metastasis. Interestingly, despite the significant and continuous tumor cell dissemination into the circulation in cancer patients, clinical observation and animal model studies indicate that metastasis is a rather inefficient process (Fidler and Kripke, 2003). This raises a debate as to whether the tendency to metastasize is largely determined by the identities of mutant alleles acquired relatively early during multistep tumorigenesis or a potential contribution from host genetic backgrounds where the local microenvironment of metastasis-susceptible sites may dictate the ability of a tumor to metastasize, or both (Bernards and Weinberg, 2002; Fidler, 1995; Hunter, 2004).

Hepatocellular carcinoma (HCC) represents an extremely poor prognostic cancer (Thorgeirsson and Grisham, 2002).

SIGNIFICANCE

The poor outcome of HCC patients results from metastases and/or postsurgical recurrence of the primary tumor. Despite considerable tumor cell dissemination, frequently observed in the hepatic venous system, metastases are rare and may be influenced by permissive target environments. Here, we demonstrate that significant gene expression changes occur in the liver microenvironment of patients with accompanying venous metastases. We reveal a unique expression signature, largely contributed by inflammation/immune responses, in noncancerous hepatic tissues with venous metastasis. This signature is a superior predictive tool to determine HCC venous metastases and relapse and may have possible utility in clinical settings to identify HCC patients who may benefit from certain postsurgical treatment to prevent metastases and/or recurrence.

The dismal outcome has been attributed to the highly vascular nature of HCC tumors, which increases the propensity to spread and invade into neighboring or distant sites (Nakakura and Choti, 2000; Tang, 2001). Intrahepatic metastases, especially venous metastases, are a major hallmark of metastatic HCC, with new tumor colonies frequently invading into the major branches of the portal vein or, to a lesser extent, the inferior vena cava and possibly other parts of the liver (Yuki et al., 1990). Another feature of HCC is a high frequency of multiple nodules that occur in the same or different lobes. Many of these lesions can be multicentric, resulting from multiple de novo tumors, and thus may not be metastases. Recently, we developed a gene expression signature specific to primary HCC specimens to predict prognosis and venous metastases (Ye et al., 2003). The tumor signature provided 78% overall accuracy in predicting HCC patients with metastatic potential. The presence of a prognostic signature in primary HCC specimens was confirmed by several studies (Iizuka et al., 2003; Lee et al., 2004). However, HCC is usually present in inflamed fibrotic and/or cirrhotic liver with extensive lymphocyte infiltration due to chronic hepatitis. Thus, it is possible that HCC metastatic propensity may be determined and/or influenced by the local tissue microenvironment of the host.

To determine the role of the hepatic microenvironment in HCC metastasis, we compared the gene expression profiles of 115 noncancerous surrounding hepatic tissues from two HCC patient groups, those with primary HCC with venous metastases (major branch of the portal vein or inferior vena cava) or confirmed extrahepatic metastases by follow-up, which we termed a *m*etastasis-*i*nclined *m*icroenvironment (MIM) sample, and those with HCC without detectable metastases, which we termed a *m*etastasis-*a*verse *m*icroenvironment (MAM) sample. Using this patient cohort, we first conducted gene expression profiling studies of a subset of MIM and MAM samples using cDNA microarray. We identified a unique change in the gene expression profiles associated with a metastatic phenotype. Furthermore, using the same subset of MIM and MAM samples used in the microarray, we constructed a refined expression signature containing 17 genes, which we determined by quantitative real-time polymerase chain reaction analyses (qRT-PCR). This signature was validated by an independent cohort of 95 MIM and MAM samples and could successfully predict both venous metastases and extrahepatic metastases by follow-up with >92% overall accuracy. Moreover, the prognostic performance of this signature was superior to and independent of other available clinical parameters for determining patient survival or recurrence including patient age, tumor size, liver function, microvascular invasion, TNM staging, etc. Analysis of the lead signature genes revealed their involvement in the cellular immune and inflammatory responses. Consistently, dramatic changes in cytokine responses, favoring an anti-inflammatory microenvironmental condition, occur in MIM samples, where a predominant Th2-like cytokine profile, favoring a humoral response, is associated with the MIM condition. CSF1 may be one of the cytokines overexpressed in the liver milieu that is responsible for this shift. We suggest that the inflammatory status of the surrounding tumor milieu, in addition to the metastatic potential of the tumor cells, may play an important role in promoting HCC tumor progression and venous metastases.

Results

The search for a metastasis signature in noncancerous hepatic tissue from HCC patients with intrahepatic venous metastases

We recently developed a metastasis signature based on the gene expression of primary HCC tumor specimens to predict metastatic HCC and prognosis with an overall accuracy of 78% (Ye et al., 2003). To analyze a potential contributing role of the liver microenvironment in promoting intrahepatic venous metastasis, we first compared the gene expression profiles of noncancerous hepatic tissues of the cases described above (9 MIM and 11 MAM samples), to a pool of eight disease-free normal livers utilizing the same microarray platform employed in our previous study (Ye et al., 2003). This approach allowed us to compare the gene expression between the primary tumor and its surrounding tissue. Using a supervised class comparison method at a significance level of $p < 0.001$, we identified 454 significant genes that can discriminate the MIM and MAM groups (Table S1, "Training set"), with a 90% probability of the first 415 genes containing no more than ten false discoveries (Table S2). We further confirmed these findings by applying a multivariate class prediction algorithm termed compound covariate predictor (CCP), with leave-one-out cross-validation and 2000 random permutations of the class label. CCP analysis was statistically significant ($p = 0.04$) in predicting these samples with 80% overall accuracy, and similar results were obtained with four additional algorithms (Table S3). Interestingly, when comparing this 454 gene signature to a 201 gene metastasis signature identified from tumor specimens of the same patients at a lesser significance level ($p < 0.002$), we found only four overlapping genes (*VAMP3*, *PDK1*, *SLC20A2*, and *RAB28*). These results indicate that the liver microenvironment signature is principally different from the tumor signature. Consistent with our previous data (Ye et al., 2003), the distinction found in noncancerous hepatic tissues between metastatic and nonmetastatic patients is also unlikely due to tumor burden because the average tumor size in the MIM group is similar to that of the MAM group (Table S4). It has been indicated that microvascular invasion (the presence of tumor cells inside the lumen of the microvasculature) may also be associated with poor prognosis. Interestingly, when we stratified these samples based on the presence or absence of microvascular invasion, we found only three significant genes ($p < 0.001$), and the results of class prediction were statistically insignificant. At such a significance level, these genes are likely false positives. Similarly, no difference in gene expression could be found when the tumor expression microarray data were used. Thus, it appears that a significant discriminatory weight can be found with venous metastases but not with microvascular invasion by the microarray-based expression profiling approach.

A hierarchical clustering of the 454 significant genes revealed that 295 genes were more abundantly expressed in MIM samples, while 159 genes were more abundantly expressed in MAM samples (Figure 1A). A close examination revealed two striking gene clusters that most significantly differentiated MIM from MAM samples. We named these two clusters inflammation/immune response cluster A and B, respectively. Cluster A contains 38 underexpressed genes, while cluster B contains 68 overexpressed genes in the MIM group. Strikingly, over 30% of the genes in these two clusters have gene annotations

associated with either inflammation and/or immune response functions (Figure 1A). For example, *HLA-DRA*, a MHC class II molecule, was most significantly upregulated in noncancerous MIM samples. Another MHC class II molecule, *HLA-DPA1*, was also highly upregulated in MIM samples.

To validate the expression level of differential genes in these samples, we selected *HLA-DRA* and *HLA-DPA1*, along with two mast cell-related genes, *PRG1* and *ANXA1* (an anti-inflammatory protein), represented in Cluster B, to perform qRT-PCR (Figure 1B), based on their involvement in immunity. The qRT-PCR analysis demonstrated that these four genes were significantly upregulated in noncancerous tissues from MIM compared to MAM samples (Figure 1B). A comparison of the expression ratios of these four genes from either microarray analysis or qRT-PCR showed a statistically significant correlation ($p < 0.0001$; $r^2 = 0.6187$) (Figure 1C). It appears that the components of the immune system may function as affecting targets of metastatic potential, and thus, this process may be influenced by the immune status of hepatic tissues.

HCC venous metastases are accompanied by changes in the immune status of the tumor-surrounding tissue microenvironment

Since the immune status of the liver microenvironment seemed to be associated with venous metastases, we next examined the status of cellular inflammation by determining the expression of an inflammatory status marker, nitric oxide synthase 2 (NOS2), using immunohistochemistry (IHC) analyses of 37 MIM and 31 MAM samples, most of which were not used in our gene expression profiling studies. NOS2 was detected in noncancerous liver parenchyma and was mainly contributed by hepatocytes (Figure 2A). It was evident that NOS2 staining was significantly different ($p = 0.009$) between MIM and MAM samples, whereby nonmetastatic liver parenchyma showed increased expression of NOS2 (Figure 2B). Since 96% of the samples (65/68) were from HBV-positive carriers and a majority of them (93%) (63/68) had underlying cirrhosis by histological evaluation, it was anticipated that the level of NOS2 would be elevated in these samples. Thus, it appears that a pro-inflammatory condition is associated with MAM samples and an anti-inflammatory condition is associated with MIM samples. However, there is no significant difference ($p = 0.570$) between the overall inflammation status of benign MIM and MAM tissues based on histological activity index (Figure S1).

We then determined whether the differences in NOS2 expression were associated with changes in certain immune cell responses in MIM samples. We randomly selected ten paraffin-embedded MIM or MAM cases, which were subjected to a panel of immune cell markers by IHC analyses. CD68 was used to monitor the abundance of resident macrophages, the Kupffer cells (one type of antigen presenting cell [APC]); HLA-DR was used to determine the activity of APC; CD45 was used to determine the total leukocyte amount; and CD4 or CD8 was used to identify the number of CD4+ or CD8+ T lymphocytes, respectively. We found a substantial increase in the numbers of CD68+ and HLA-DR+ cells in noncancerous liver parenchyma (away from the portal tract) in patients with metastatic HCC (Figures 2A, 2C, and 2D). All of the CD68+ and HLA-DR+ cells were localized to the liver sinusoid (Figure 2A), the main site of Kupffer cells; liver-associated lymphocytes; and liver sinusoidal endothelial cells. There is a significant correlation in staining between CD68 and HLA-DR among these cases (Figure 2E; $p = 0.0003$; $r^2 = 0.5285$), indicating that the difference between MIM and MAM samples is unlikely due to a sampling bias in the staining area used for quantitation. Interestingly, most of the HLA-DR+ cells appear to overlap with CD68+ cells in MAM samples, while many more HLA-DR+ cells were evident in MIM samples when compared to CD68+ cells (Figures 2A and 2E; Figure S2), suggesting that many of the HLA-DR+ cells are contributed by an APC cell type other than Kupffer cells. Most of the HLA-DR+ cells appear to overlap with CD45+ cells in MIM samples, suggesting that the microarray-identified *HLA-DRA* signal is mainly contributed by leukocytes (Figure S3). The number of CD4+ and CD8+ T cells is much lower in the areas where HLA-DR+ and CD68+ cells are found, and they are mainly localized in the portal tract where extensively circulating infiltrating lymphocytes can be found (data not shown). In addition, we also examined the expression of CSF1, a major cytokine regulating the activity of tissue macrophages (Pixley and Stanley, 2004). Similar to NOS2, CSF1 staining is mainly confined to hepatocytes of noncancerous liver parenchyma, which can be detected more frequently in MIM compared to MAM samples with a borderline statistical significance ($p = 0.078$) (Figure 2F and Figure S3). A significant increase in the abundance of CSF1 mRNA in MIM samples ($p < 0.0003$) was confirmed by qRT-PCR analysis of noncancerous liver tissues of the original 9 MIM and 11 MAM samples (Figure 2G). It is plausible that the increase in HLA-DR+ cells, accompanied by the increase in Kupffer cells, may be due, in part, to an elevation of CSF1.

The MIM group is associated with an increase in Th2 cytokines and a decrease in Th1 cytokines

Our gene expression results showed a distinct effect on immune and inflammatory responses in MIM samples, which were corroborated by IHC analysis showing an increase in liver macrophages and a decrease in NOS2 expression in samples belonging to this group. Pro-inflammatory cytokines, such as IL1, TNFα (TNF), and IFNγ (IFNG) have also been shown to induce NOS2 expression (Paludan et al., 2001; Spirli et al., 2003). Consequently, we analyzed the cytokine profile of the 9 MIM and 11 MAM samples used in the microarray analysis by qRT-PCR using the Taqman Cytokine Gene Expression Plate, composed of 12 cytokines belonging to either Th1 or Th2 families. Strikingly, MIM samples showed a profound switch in their cytokine profiles, with a significant increase in *IL4*, *IL5*, *IL8*, and *IL10* (Th2 cytokines) and a concomitant decrease in *IL1A*, *IL1B*, *IL2*, *IFNG*, and *TNF* (Th1 cytokines) compared to a normal liver pool (Figures 3A and 3F). However, such a switch was not evident in MAM samples, where the profiles were similar to cirrhosis liver samples from chronic HBV carriers, primary biliary cirrhosis (PBC), or autoimmune hepatitis (AIH) (Figures 3B–3E). Thus, such a profound cytokine profile switch is unique to hepatic tissues from metastatic HCC patients and is unlikely due to the degree of viral hepatitis or the status of cirrhosis as evidenced by the lack of this profile in HBV, AIH, or PBC samples, nor is it a consequence of tumor burden since this profile is not observed in HBV-positive MAM samples. The observed induction of inflammatory cytokines in MAM samples, such as *IFNG* and *TNF*, is consistent with an increase of inflammation as evidenced by NOS2 and suggests that the inflammatory status of the liver microenvironment may retard venous metastases. Taken together, these data imply

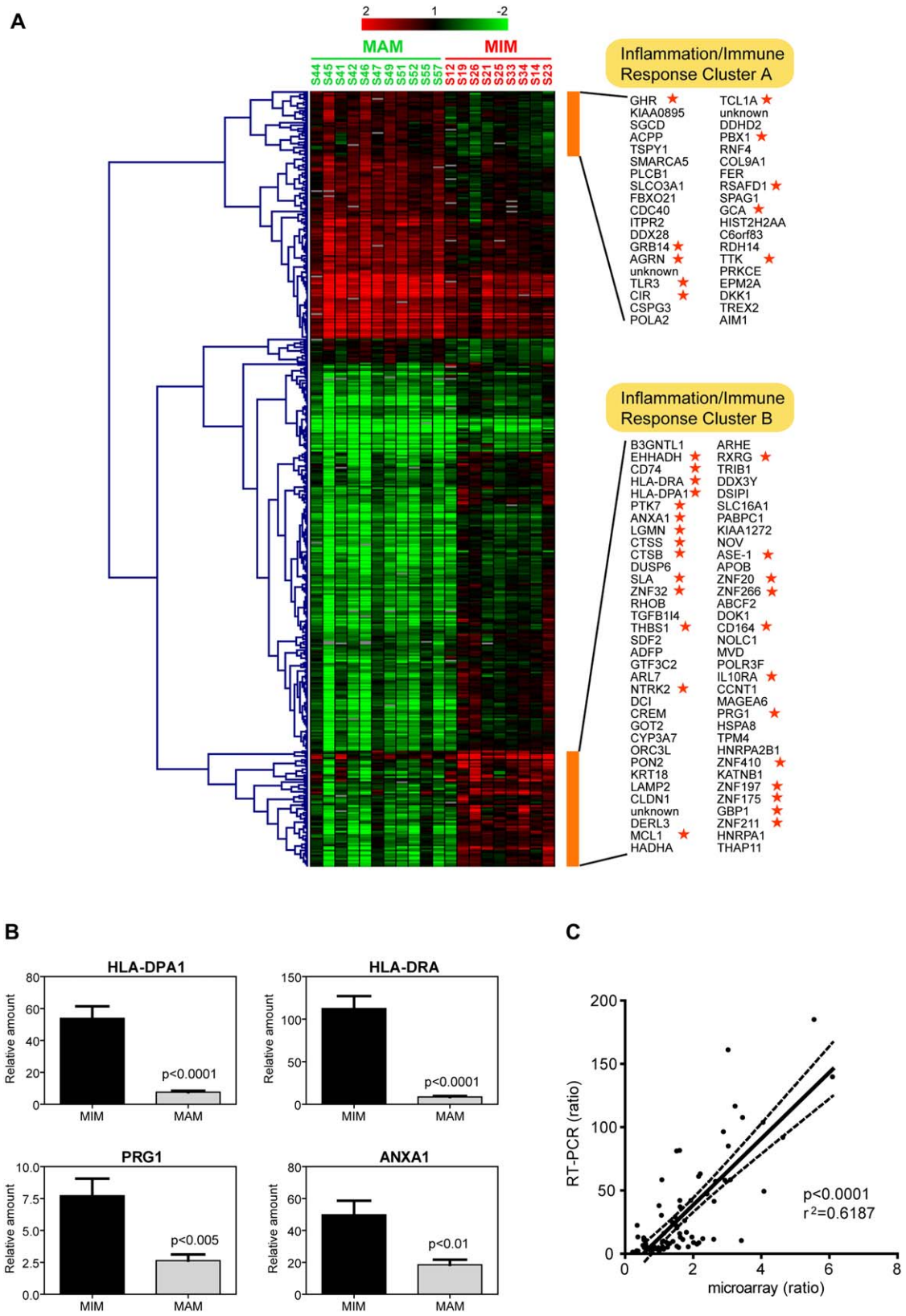

Figure 1. Significant differentially expressed genes in noncancerous hepatic tissues from MIM and MAM patients

A: Hierarchical clustering of 454 genes whose expression was significantly ($p < 0.001$) altered in the metastatic (MIM) samples ($n = 9$) and nonmetastatic (MAM) samples ($n = 11$) from class prediction analysis with six different algorithms employing leave-one-out cross-validation to establish prediction accuracy. Each row represents an individual gene, and each column represents an individual tissue sample. Genes were ordered by Euclidian distance and complete linkage according to the ratios of abundance in each tissue sample compared to a normal tissue pool ($n = 8$), which were normalized to the mean abundance of

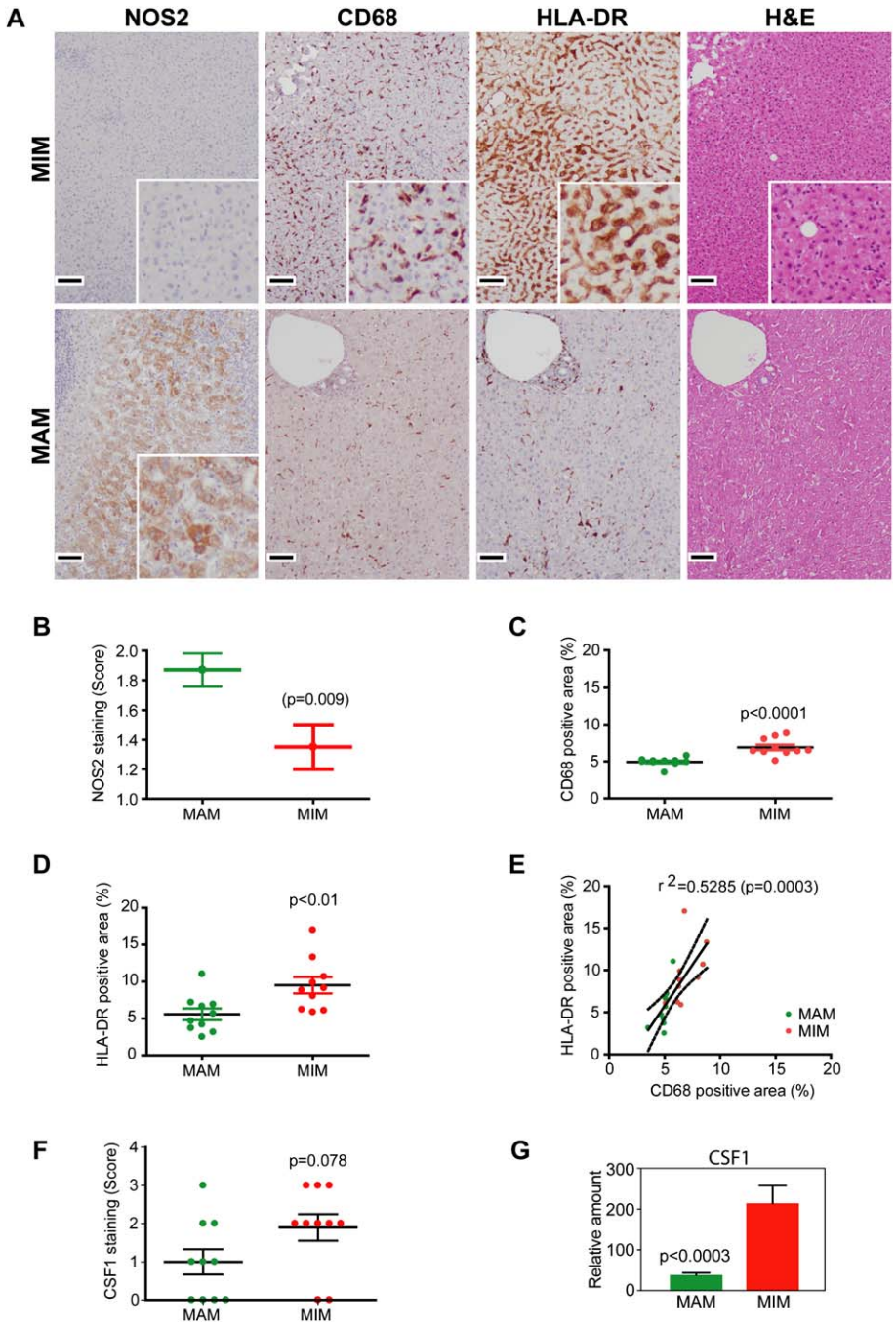

Figure 2. Metastatic potential is associated with changes in immune cell expression and inflammatory status

A: Five micrometer sections of paraffin-embedded hepatic tissues from a representative MIM and a MAM case immunostained for NOS2, HLA-DR, CD68, or H&E are shown. Boxes in the right corner show magnified images (magnification ×5). The horizontal black bar represents 50 μm. **B:** NOS2 staining was quantified for original samples and an additional cohort of HCC samples (MIM: n = 37, MAM: n = 31) based on blinded-histological scoring determined by both the intensity and distribution of NOS2 expression. Quantitation of HLA-DR (**C**) or CD68 (**D**) was based on ten randomly selected MIM or MAM samples with marker expression in liver parenchymal regions without inflamed regions such as the portal tract and central vein. Data (**B** and **D**) are shown as the mean ± SEM, and the statistical significance was calculated from the Student's t test between MIM and MAM samples. **E:** Pearson correlation analysis of HLA-DR versus CD68 staining. **F:** CSF1 staining was quantified in a similar fashion to NOS2 described above. **G:** qRT-PCR of CSF1 was performed as described in Figure 1B.

that an anti-inflammatory status occurs in patients with metastatic HCC.

To determine if such a profound switch in Th1-Th2 cytokine profiles was contributed by an abnormal expression of CSF1, we first examined the serum concentration of CSF1 in an independent cohort of 57 patients (10 noncancerous [NC], 33 MAM samples, and 14 MIM) by ELISA. NC samples were cancer-free HBsAg carriers, defined as patients collected from the same region as the HCC cases without any detectable tumors at the time of sample collection. Although MAM samples showed a significant elevation of serum CSF1 when compared to NC samples ($p < 0.02$), the level of CSF1 is significantly higher in MIM samples

genes. Pseudocolors indicate transcript levels below, equal to, or above the mean (green, black, and red, respectively). Missing data are denoted in gray. The scale represents the gene expression ratios from 2 to −2 in log 2 scale. Inflammation/immune response clusters are denoted by the vertical orange bars. Genes known to be related to the immune and inflammation responses are denoted by the red stars.

B: qRT-PCR validation of significant differentially expressed genes. Relative expression fold of each gene (n = 4) normalized to 18S and a normal tissue pool is shown for *HLA-DRA*, *HLA-DPA1*, *ANXA1*, and *PRG1*. Data are presented as the mean ± SEM, and the statistical significance calculated from the Student's t test between MIM and MAM samples is shown.

C: Pearson correlation analysis between microarray and qRT-PCR ratios of abundance data for the four validated genes described in **B** is shown.

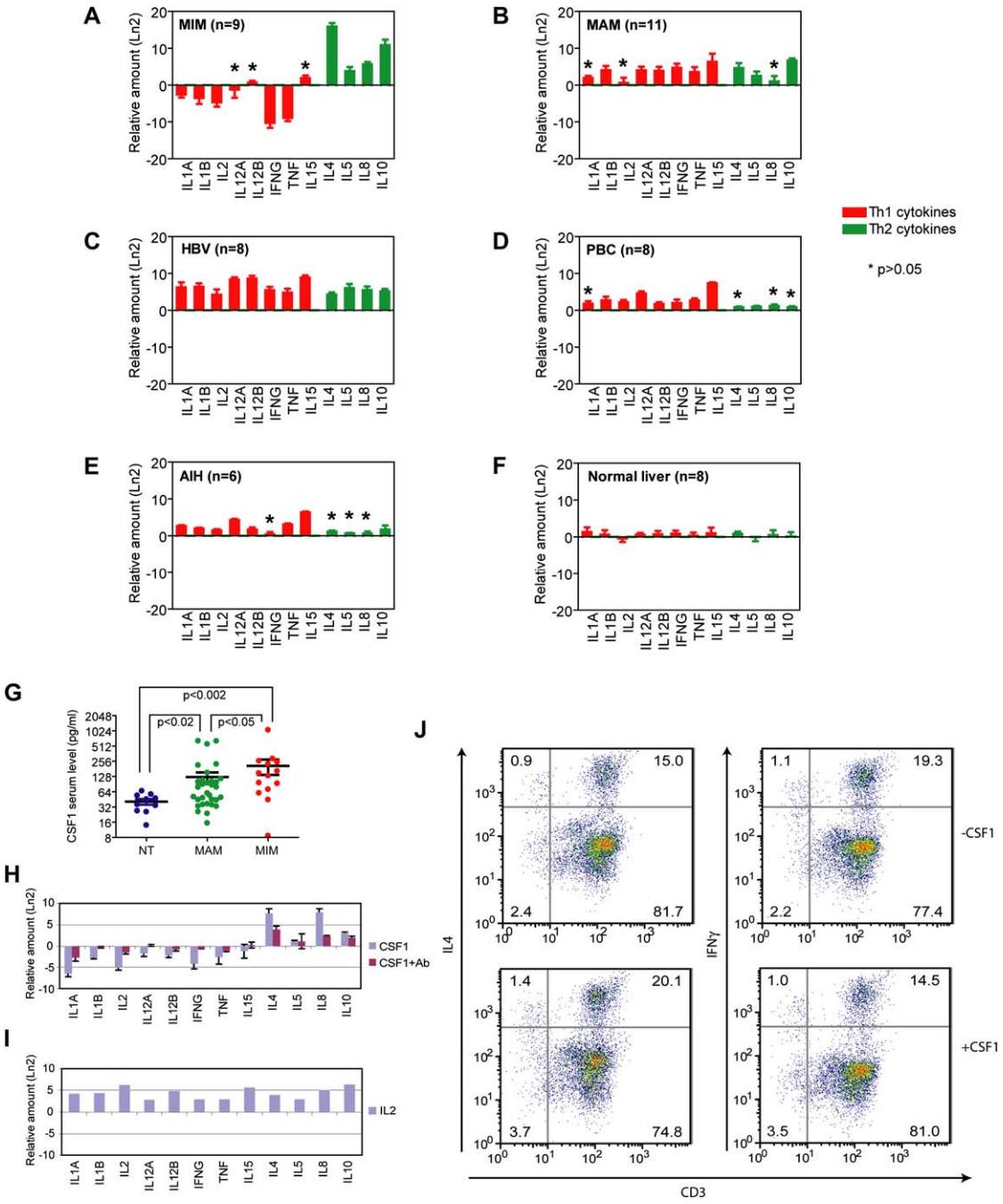

Figure 3. Metastatic potential is associated with a reprogramming of Th1 and Th2 cytokines in noncancerous hepatic tissues

The cytokine expression profiles of MIM (**A**), MAM (**B**), HBV (**C**), PBC (**D**), AIH (**E**), and normal liver (**F**) samples are shown. qRT-PCR was conducted using the Taqman Cytokine Gene Expression plate (Applied Biosystems, Foster City, CA). The natural log value of cytokine quantity, normalized to 18S rRNA and to a normal liver tissue pool (n = 8), is presented as the mean ± SD (standard deviation). Statistically insignificant changes calculated by the Student's t test ($p > 0.05$) relative to normal liver are denoted by asterisks. **G–I:** CSF1 is more abundant in serum from metastasis patients and can modulate the expression of Th1 and Th2 cytokines, correlating with metastasis cytokine profiles. **G:** ELISA-based quantitation of the level of CSF1 in human serum from normal liver, MAM, or MIM. Data are presented as the mean ± SEM, and the statistical significance calculated by a nonparametric test (Mann-Whitney test) among samples is shown. **H:** The cytokine expression profiles of peripheral blood mononuclear cells (PBMC) isolated from buffy coat and treated with CSF1 (2 ng/ml), CSF1 blocking antibody (30 ng/ml), or IL2 (50U) (**I**) are shown. **H and I:** Cytokine quantity, normalized to 18S rRNA and BSA treatment, is presented as the mean in log 2 scale of abundance ± SD (n = 3). **J:** Human PBMC (2×10^6 cells) was treated with CSF1 (2 ng/ml) for 24 hr followed by treatment with PMA (25 ng/ml) and Calcium Ionophore (1 μg/ml) for 2 hr and GolgiPLUG (BrefeldinA) for 2 hr. Cells were harvested, stained with FITC-CD3, fixed, permeabilized, treated with serum, and subsequently stained for the intracellular cytokines APC-IL4 or APC-IFNG. The percentage of cells in each quadrant are shown.

($p < 0.002$), and the difference between MIM and MAM samples is evident ($p < 0.05$) (Figure 3G). The average serum concentrations of CSF1 are 40.7 ± 5.1 pg/ml in NC (±SEM; standard error), 124.6 ± 28.9 pg/ml in MAM, and 207.5 ± 70.0 pg/ml in MIM, respectively. Next, to determine the effect of CSF1 on cytokine profiles, we utilized peripheral blood mononuclear cells

(PBMC) isolated from healthy donors as a model system, an immune cell-enriched source to mimic the immune response in hepatic tissue. We found that, similar to the effect seen in MIM samples, PBMC incubated with recombinant CSF1 in a physiologically relevant concentration resulted in a significant increase in Th2 and a decrease in Th1 cytokines (Figure 3H). As a control, recombinant IL2 led to an increase in all cytokines (Figure 3I). The CSF1 effect can be observed in PBMC from at least three healthy donors tested and is specific to CSF1 since its activity can be effectively reduced by a CSF1 neutralizing antibody. To address the cell type affected by CSF1 to induce the cytokine profile shift noted above, we determined the intracellular concentration of IL4 and IFNG by fluorescence-activated cell sorting (FACs) (Figure 3J). We found that, in cells labeled with CD3, a cell surface marker for T cells, CSF1 increased the amount of the Th2 cytokine IL4 by 30% and reduced the levels of the TH1 cytokine IFNG by 30%. It should be noted that a small fraction of CD3-negative cells also apparently induce a shift toward Th2 in the presence of CSF1.

Composition and predictive value of a refined venous metastasis signature using noncancerous hepatic tissues

Our results thus far showed that 454 genes could distinguish MIM and MAM samples by microarray, and a significant amount of these genes were related to the immune/inflammatory response. However, we were inclined to accurately differentiate these samples using a smaller, more defined set of genes and a more rapid profiling methodology, namely qRT-PCR, for potential clinical utilization. Consistently, qRT-PCR profiling of 9 MIM and 11 MAM samples used in the microarray study revealed that 17 immune/inflammatory related genes, which we refer to as the refined liver microenvironment venous metastasis signature (12 Th1/Th2 cytokines, *HLA-DR*, *HLA-DPA*, *ANXA1*, *PRG1*, and *CSF1*), were sufficient to discriminate MIM from MAM samples (Figure 4A; Table 1). Hierarchical clustering of 9 MIM, 11 MAM, and 8 normal liver samples based on the expression of these 17 genes by qRT-PCR resulted in a clear separation of these three groups, with MIM showing a more dramatic expression difference when compared to MAM and normal liver samples (Figure 4A). Thus, these 17 genes may provide a unique signature to classify patients with venous metastases by examining only noncancerous liver tissues (Table 1).

To analyze the prediction accuracy of this 17 gene signature, we first tested the probability of correctly classifying the original 9 MIM and 11 MAM samples as a training set by the *p*rediction *a*nalysis of *m*icroarrays (PAM) algorithm. PAM analysis, utilizing nearest shrunken centroid classification with 10-fold cross-validation, resulted in 100% correct classification of these samples into either the MIM or MAM group (Figure 4B). To further validate our results, we performed qRT-PCR of the 17 gene signature set on a testing cohort comprised of an additional 95 noncancerous liver specimens (43 MIM and 52 MAM) (Table S1, ''Testing set''). These independent samples had similar clinical profiles as the original 20 samples used in training, except for some differences in tumor morphology scores (Table S1). The MIM testing cohort was comprised of 21 samples with metastases found in the portal vein (n = 30), inferior vena cava (n = 6), or common bile duct (n = 5) at the time of sample collection, and 11 samples with extrahepatic metastases confirmed by follow-up, of which 10 also had intrahepatic metastases. Prediction analysis revealed that the 17 gene signature correctly predicted 38 of 43 MIM cases (88%) and 49 of 52 MAM cases (94%) (Figure 4C). Importantly, this signature was capable of accurately predicting 7 of 11 MIM cases (64%) where venous metastases were not present at the time of sample collection but developed at follow-up. To further test if there was any grouping bias in training and testing, we performed PAM analysis with 10-fold cross-validation for all 115 cases. Consistently, this analysis resulted in a 93% overall correct classification with eight misclassified cases (data not shown). A close examination of the clinical characteristics of the eight misclassified cases (three MAM and five MIM) did not reveal any reason for misclassification (Table S5). In addition, the 17 gene signature was an excellent predictor of patient recurrence within this cohort (79% sensitivity and 67% specificity). It should be noted that, among the 115 HCC cases, 99% had a history of HBV infection and a majority were chronic HBV carriers (Table S6). In addition, the number of cases with a marker of active viral replication (HBeAg+) was similar between metastatic and nonmetastatic groups (Table S6). Thus, it appears that HBV viral load does not seem to contribute to the metastatic changes in the local hepatic microenvironment.

To determine if the signature was related to patient prognosis, we performed Kaplan-Meier survival or recurrence analysis based on the 17 gene prediction results (Figure 4D). It appeared that the predicted metastatic group had a significantly shorter survival period when compared to the nonmetastatic group ($p = 4.2e\text{-}11$). Kaplan-Meier analysis also showed that the predicted metastatic group had a significantly shorter period for recurrence than the nonmetastatic group (Figure 4D; $p = 0.0002$). Thus, this signature provides weight to predict both survival and recurrence. As shown by multidimensional scaling analysis, samples from the MIM group clustered separately from samples without venous metastases demonstrating measurable differences between these two populations (Figure 4E). Interestingly, the eight misclassified cases are close to but do not overlap with the assigned groups, suggesting that unknown clinical conditions, not a problem of the signature, may be responsible for these misclassifications. It should be noted that these outcome data were accessed at a 3 year follow-up, and thus the prediction accuracy of this signature will have to be reassessed to determine whether it can still accurately predict patient survival and recurrence at longer follow-up periods.

Since several clinical parameters have been shown to correlate with HCC prognosis, we further determined whether the metastatic HCC predictor was confounded by underlying clinical conditions by performing univariate and multivariate Cox proportional hazards regression analysis. A univariate analysis of various clinical variables in the cohort revealed that α-fetoprotein (AFP), albumin, Child-Pugh score, and several staging systems (TNM, CLIP, BCLC, and Okuda) were significant predictors of survival. However, the 17 gene predictor was far superior (a hazard ratio of 9.2) to other clinical variables (hazard ratio of 5.3 or less) (Table 2). A univariate analysis also revealed that none of the clinical variables tested were significant predictors of recurrence; however, the 17 gene predictor was significantly associated with this outcome ($p = 0.001$) (Table 2). In the univariate recurrence analysis, tumor differentiation could not be analyzed due to the small sample size within this cohort after stratification. Tumor size was not a significant predictor at either 5 cm or 3 cm (Table 2 and data not shown). The multivariate Cox regression model for survival, which controlled for HBV status, ALT,

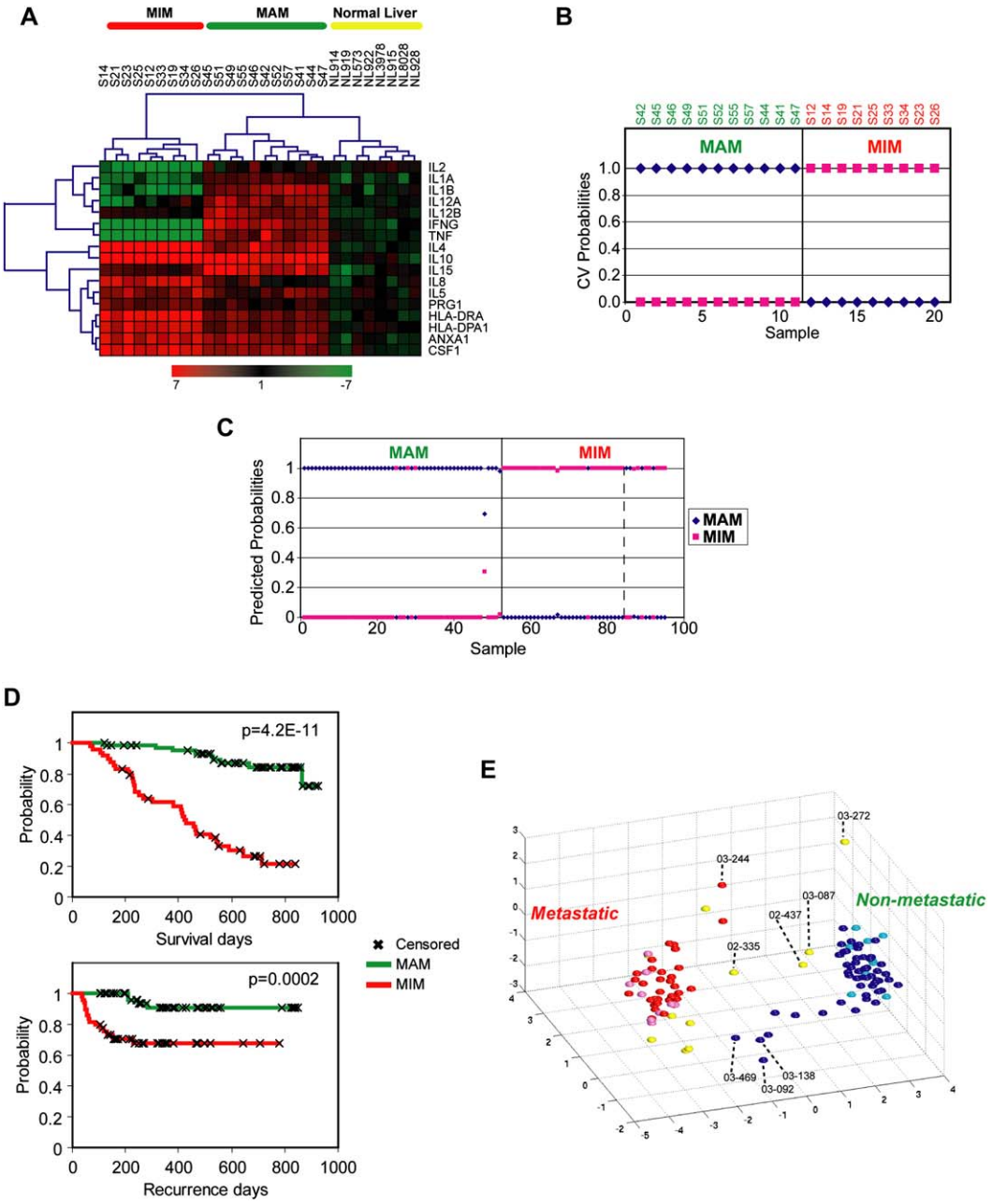

Figure 4. qRT-PCR-based differential expression of signature genes and Th1-like or Th2-like cytokines can distinguish samples with metastatic potential

A: qRT-PCR was conducted on individual noncancerous (NC) samples (n = 8) and MIM (n = 9) or MAM (n = 11) samples. Cytokine or signature gene quantity was normalized to 18S rRNA and to a normal tissue pool (n = 8). Genes and samples were ordered by Euclidian distance and complete linkage according to the ratios of abundance in each tissue sample compared to a normal tissue pool (n = 8). Pseudocolors indicate transcript levels above (red), below (green), or equal to (black) the mean, respectively. The scale represents the gene expression ratios from 7 to −7 in log 2 scale.

B: PAM analysis of MIM (n = 9; pink squares) and MAM (n = 11; blue diamonds) samples used in the training set.

C: PAM analysis of an additional 95 samples (52 MAM and 43 MIM). The 11 samples on the right side of the dotted line within the MIM-defined box represent those solitary HCC with venous metastases confirmed at follow-up.

D: Kaplan-Meier recurrence or survival analysis of metastatic and nonmetastatic samples based on the results of PAM classification.

E: Multidimensional scaling of training samples (MIM, pink; MAM, light blue) and testing samples (MIM, red; MAM, dark blue; MIM with venous metastases confirmed at follow-up, yellow) based on Euclidian distance of the expression of the 17 gene signature. Labeled circles represent misclassified samples.

Child-Pugh score, microvascular invasion, and tumor differentiation showed a 15.1 increased risk of death for those with the MIM expression profile compared with that of MAM (Table 2). Although Child-Pugh score showed a significant association with death in metastatic compared to nonmetastatic samples ($p = 0.014$), the predictor was most significantly associated with this outcome for samples with the MIM profile ($p < 0.001$). A further evaluation of the significant weight of CLIP, BCLC, and Okuda staging in a multivariate model was not performed due to missing data for these covariates (n = 86). The multivariate Cox regression model for recurrence which controlled for HBV status, AFP, and albumin showed a 7.9 increased risk of

Table 1. Description of the 17 gene metastasis signature derived from noncancerous hepatic tissues

Gene symbol	Gene name	Unigene ID	Function	Source of cells
IL1A	interleukin 1, α	Hs.1722	activates T and B cells and monocytes	T or B cells, monocytes, macrophages
IL1B	interleukin 1, β	Hs.126256	activates T and B cells and monocytes	T or B cells, monocytes, macrophages
IL2	interleukin 2	Hs.89679	growth and differentiation of all immune cells	T cells
IL12A	interleukin 12, p35	Hs.673	stimulates Th1 T cells; induces IFNγ; defense against pathogens	B cells, monocytes, macrophages
IL12B	interleukin 12, p40	Hs.674	stimulates Th1 T cells; induces IFNγ; defense against pathogens	B cells, monocytes, macrophages
IL15	interleukin 15	Hs.311958	similar to IL-2; stimulates T cell proliferation	monocytes
IFNG	interferon γ	Hs.856	monocyte activator; regulates immune and inflammatory responses	T cells, macrophages, NK cells
TNF	tumor necrosis factor	Hs.241570	mediator of inflammatory and immune functions	T or B cells, monocytes, macrophages
IL4	interleukin 4	Hs.73917	induces secretion of Ig by B cells; pleiotropic effect on T cells	T or mast cells
IL5	interleukin 5	Hs.2247	differentiation factor for B cells and eosinophils	T or mast cells
IL8	interleukin 8	Hs.624	angiogenic factor; activating factor for neutrophil; attracts basophils	T or B cells, monocytes
IL10	interleukin 10	Hs.193717	blocks Th1 T cells cytokines; stimulates proliferation of B cells, thymocytes, and mast cells; stimulates IgA production by B cells	T or B cells, monocytes
CSF1	colony-stimulating factor	Hs.173894	stimulates the proliferation, differentiation, and survival of monocytes, macrophages	epithelial cells, fibroblasts, endothelial cells
ANXA1	annexin A1	Hs.494173	anti-inflammatory, capable of decreasing leukocyte migration	monocytes, neutrophils
HLA-DRA	MHC class II antigen	Hs.520048	antigen presentation	dendritic, B, epithelial, or endothelial cells, macrophages, fibroblasts
HLA-DPA1	MHC class II antigen	Hs.347270	antigen presentation	dendritic, B, epithelial, or endothelial cells, macrophages, fibroblasts
PRG1	platelet proteoglycan	Hs.1908	involved in packaging of proteins into secretory granules and/or directing the secretion of such molecules as cytokines or chymases	hematopoietic cells, endothelial cells

recurrence for those with the MIM expression profile compared with that of MAM (Table 2). Although HBV status showed a borderline significant association with death in metastatic compared to nonmetastatic samples ($p = 0.053$), the MIM-MAM signature was a far better predictor of patient recurrence ($p < 0.001$). These results show that the predictor was by far the strongest prognosticator for both patient survival and recurrence when compared to any of the clinical variables analyzed.

Discussion

A major hallmark of an aggressive solitary HCC is its ability to metastasize. Understanding the mechanisms underlying this process would allow for the development of effective approaches to reduce HCC-related mortality. Our recent studies indicate that the gene expression signature of primary HCCs is very similar to that of their corresponding metastases (Ye et al., 2003). In contrast, the gene expression signature differs significantly between metastasis-free primary HCCs and HCCs with accompanying intrahepatic metastases (Ye et al., 2003). These results are consistent with our findings that the HCC metastasis signature is independent of tumor size, tumor encapsulation, and patient age. A recent study on colon cancer metastasizing to the liver is consistent with our findings (D'Arrigo et al., 2005). In this study, we have demonstrated that livers bearing metastatic HCC also have a significantly different gene expression profile when compared to the livers bearing nonmetastatic HCC, and this difference is also independent of tumor size. Although these two signatures are uniquely different, both provide sufficient weight to predict metastatic HCC and survival. These results are consistent with the clinical presentations of metastatic HCC patients who have a propensity to develop intrahepatic metastases even after a curative resection. Our findings support many published studies on tumor and stroma interaction (Mueller and Fusenig, 2004), which suggest that the metastatic propensity of HCC both is inherent to the tumor cell and is influenced by the local environmental status of metastatic sites. Evidence for tumor influence in cancer progression has been shown in recent publications demonstrating the influence of tumor-infiltrating lymphocytes in follicular lymphoma and the role of tumor-educated macrophages in breast carcinoma (Dave et al., 2004; Pollard, 2004). The microenvironment receptivity of the patients in this study could therefore be influenced by factors produced by the neighboring primary HCC tumor. On another token, an individual's genetic constitution may also play an important role in affecting elements of the immune system and generating tumor-promoting effects (Hunter and Crawford, 2006). In fact, many cytokine polymorphisms are functionally related to HCC. It is possible that the changes in the microenvironment in MIM and MAM cases may be a consequence of differing genetic factors that dictate HCC metastatic susceptibility. The specific roles of primary tumors or genetic imbalances in "priming" the receptiveness of the liver microenvironment to HCC metastasis remain to be determined. It should also be noted that the identified predictor is only applicable at the present time for surgically eligible HCC patients because only about 20% of HCC patients are

Table 2. Univariate and multivariate analyses of factors associated with survival and recurrence

	Survival				Recurrence			
	Univariate analysis[a]		Multivariate analysis[b]		Univariate analysis		Multivariate analysis	
Clinical variable	Hazard ratio (95% CI[c])	p value	Hazard ratio (95% CI)	p value	Hazard ratio (95% CI)	p value	Hazard ratio (95% CI)	p value
MIM/MAM predictor (MIM versus MAM)	9.2 (4.2–20.0)	<0.001[g]	15.1 (5.0–45.8)	<0.001[g]	6.2 (2.1–18.8)	0.001[g]	7.9 (2.5–25.0)	<0.001[g]
Age (≥50 year versus <50 year)	1.0 (0.5–1.8)	0.967	n.a.[f]		0.8 (0.3–1.9)	0.559	n.a.	
Sex (male versus female)	3.3 (0.8–13.7)	0.100	n.a.		2.6 (0.4–19.7)	0.100	n.a.	
HBV (AVR-CC versus CC)[d]	0.9 (0.4–2.1)	0.735	0.9 (0.3–2.4)	0.796	2.3 (0.9–5.9)	0.100	3.5 (1.0–12.4)	0.053
AFP (≥300 ng/ml versus <300 ng/ml)	2.0 (1.0–3.7)	0.038[g]	n.a.		2.2 (0.9–5.1)	0.102	2.9 (0.8–9.8)	0.089
ALT (≥50 U/l versus <50 U/l)	1.0 (0.5–2.0)	0.945	0.6 (0.3–1.4)	0.234	1.0 (0.4–2.4)	0.964	n.a.	
Albumin (≥0.15 g/l versus >0.15 g/l)	0.3 (0.1–0.6)	0.001[g]	n.a.		1.1 (0.3–3.7)	0.902	1.9 (0.5–6.8)	0.326
Child-Pugh score (B versus A)	2.9 (1.0–8.4)	0.049[g]	5.2 (1.4–19.1)	0.014[g]	1.5 (0.4–6.6)	0.581	n.a.	
Tumor size (≥3 cm versus <3 cm)	2.0 (0.7–5.1)	0.157	n.a.		1.3 (0.4–4.3)	0.711	n.a.	
Tumor encapsulation (none versus complete)	2.2 (1.0–4.6)	0.053	n.a.		3.7 (0.7–16.1)	0.079	n.a.	
Microvascular invasion (yes versus no)	2.1 (1.1–3.9)	0.024[g]	1.1 (0.6–2.1)	0.841	2.3 (0.9–6.0)	0.071	n.a.	
TNM stage (II + III versus I)[e]	2.9 (1.4–6.1)	0.024[g]	n.a.		2.8 (0.6–11.9)	0.176	n.a.	
CLIP stage (2 + 3 + 4 versus 0 + 1)	5.3 (2.5–11.4)	<0.001[g]	n.a.		1.9 (0.7–5.1)	0.186	n.a.	
BCLC stage (B + C versus 0 + A)	5.3 (2.4–11.4)	<0.001[g]	n.a.		1.8 (0.7–4.8)	0.228	n.a.	
Okuda stage (1 versus 0)	2.9 (1.4–6.1)	0.006[g]	n.a.		1.3 (0.4–3.9)	0.664	n.a.	
Tumor differentiation (II versus I–II)	0.7 (0.2–2.5)	0.628	1.1 (0.2–8.4)	0.906	n.a.		n.a.	
Tumor differentiation (II–III + III + IV versus I–II)	1.1 (0.3–3.7)	0.904	2.7 (0.3–26.5)	0.401	n.a.		n.a.	

[a]Univariate analysis, Cox proportional hazards regression.
[b]Multivariate analysis, Cox proportional hazards regression.
[c]95% CI, 95% confidence interval.
[d]CC, chronic carrier; AVR-CC, active viral replication chronic carrier.
[e]Stages II and III were combined because of the presence of vascular invasion at these stages.
[f]n.a., not applicable.
[g]Significant.

currently qualified for resection. In addition, due to the predominant HBV+ status of this cohort, it remains to be determined whether this signature is suitable for HCC patients with other underlying liver diseases such as those related to hepatitis C and/or alcohol.

Our results indicate that the hepatic microenvironment from patients with HBV-positive metastatic HCC have a profound change in their gene expression profiles. The two significant clusters in the profile reveal notable changes associated with genes whose products are involved in immune function. In fact, over 30% of the genes in these clusters are known to be related to this process. Moreover, the pro-inflammatory cytokines such as *TNF*, *IFNG*, and *IL1* are significantly downregulated while the anti-inflammatory cytokines such as *IL4*, *IL5*, *IL8*, and *IL10* are highly elevated in livers with metastatic HCC. It is known that TNF and IFNG are involved in the activation of cytotoxic T lymphocytes to induce tumor killing, whereas elevated levels of IL4 and IL10 are reported to be associated with poor prognosis of cancer (Berghella et al., 2002; Hattori et al., 2003). Consequently, TNF and IFNG have been used in several clinical trials with a measurable effect on metastatic tumors (Smyth et al., 2004). Our findings that hepatic tissues from metastatic HCC patients have a global decrease in the production of pro-inflammatory Th1-like cytokines and a more pronounced global increase in the production of anti-inflammatory Th2-like cytokines are consistent with the hypothesis that a unique immunological profile is activated to promote HCC metastases. Although many immune cell types can produce and be activated by cytokines, T cells are the predominant cell type involved in this process. Our results show that the T cell population, assayed by CD3 marker expression, is involved in the promotion of Th2 cytokines and repression of Th1 cytokines in PBMC induced by CSF1. T cells function in innate immunity in two distinct types, CD4+ T helper cells and CD8+ cytotoxic T cells (CTL). Although the CD4+ and CD8+ populations do not seem to differ in number between MIM and MAM samples (data not shown), it is possible that these populations are differentially primed in prometastatic conditions, in part by the activity of CSF1, and thus produce cytokine profiles that favor cancer advancement. The experimental results with T cells, however, do not rule out the possibility that other CD3-positive cell populations promote Th2. A NK cell subclass, termed NKT, that is abundant in the liver and represents approximately 10% of human PBMC, expresses cell surface markers for T (CD3) and NK cells (CD56) (Van Dommelen and Degli-Esposti, 2004). These cells have been implicated in detrimental immune responses and hepatic injury and could play a role in skewing cytokine responses through excessive IL4 production (Golden-Mason and Rosen, 2006; Johansson et al., 2006; Johnson et al., 2002). Moreover, in general, natural killer (NK) cells produce a range of cytokines and are required to activate CTLs and CD4+ T cells and thus initiate T cell responses (Zingoni et al., 2005). Our data show that NK cells are also involved in Th2 promotion in PBMC treated with CSF1 (data not shown). Further experiments are warranted to analyze the role of hepatic NK and NKT cells in the cytokine profile imbalances that occur with venous metastases.

Inflammation is known to be closely associated with cancer development (Coussens and Werb, 2002; de Visser and Coussens, 2005; Hussain et al., 2003; Mann et al., 2005). For example, inflammation can result in an increase in nitric oxide production by NOS2, which in turn activates a p53-mediated tumor suppressive pathway (Ambs et al., 1998; Hofseth et al., 2003). Thus, the predominant humoral cytokine response in the liver milieu suggests that shifts to anti-inflammatory/immune-suppressive

responses may play a significant role in promoting HCC venous metastases. This is supported by our observation that the number of hepatic macrophages are increased in livers bearing metastatic HCC, which coincides with an increase in HLA-DR-positive cells and a decrease in NOS2 expression. Our results show that a CD3-negative population is also involved in CSF1-induced production of anti-inflammatory Th2 cytokine that may promote HCC venous metastases. Macrophages can respond to microenvironmental signals with distinct functional polarization programs, which regulate the influx of other immune cells, such as T lymphocytes, by producing a variety of cytokines and chemokines (Mantovani et al., 2002). Increased evidence indicates that tumor-associated macrophages (TAM) can polarize toward a type II phenotype, which is oriented toward tissue remodeling and repair, a process that may be compatible with metastatic progression (Pollard, 2004). Our results indicate that the Th1 to Th2-like profile switch in livers bearing metastatic HCC are accompanied by an overexpression of CSF1, as well as MHC class II-related genes, and many other immune cell-related genes including PRG1 and ANXA1, which are consistent with the hypothesis that a unique immunological condition regulated by Kupffer cells may promote HCC metastases. These findings are reminiscent of the TAM phenotype described above, whereby macrophages are ''alternatively activated.'' Consistently, CSF1, an activator and regulator of macrophages, can induce the Th1 to Th2-like profile switch in PBMC from healthy blood donors. We refer to this unique Th2-like profile associated with venous metastasis-susceptible (MS) condition of the liver as MS-Th2 and the Th1-like profile associated with a venous metastasis-unsusceptible (MU) condition as MU-Th1. Stratifying HCC patients according to MS-Th2 or MU-Th1 profiles may allow for better classification of these patients for treatment.

In this study, we have found that the 17 gene signature provides greater than 92% accuracy in correctly predicting venous metastases of an independent HCC cohort. Remarkably, this signature can also predict distant metastases developed several years later after resection. The 17 gene expression profile is also capable of significantly distinguishing patients who are likely to experience recurrence after curative resection (79% sensitivity). Although we have already identified a tumor signature capable of predicting HCC venous metastases, the microenvironmental signature outweighs the former's prediction accuracy (78% versus 93%). Importantly, the immune-related signature can also predict recurrence and was tested in a much larger cohort than our former tumor-based HCC predictor and included prediction tests of independent validation samples. It should be noted, however, that the tumor signature utilized tumor specimens that were ground to extract RNA, and hence there may have been some contribution from the microenvironment surrounding these samples. However, this would represent a small proportion of the total tumor specimen and therefore would not significantly overlap with the microenvironment signature presented in this study. Interestingly, the prognostic markers identified in a recent microarray study analyzing survival prediction in follicular lymphoma do not overlap with microenvironment immune signature in this study, suggesting that the prognostic genes may differ among different tumor types (Dave et al., 2004). It should also be noted that the 17 gene venous metastasis signature was solely based on qRT-PCR analysis, whereas the HCC tumor signature was based on microarray results. The qRT-PCR approach appears to be superior in accurately predicting an independent cohort of HCC patients with or without metastases when compared to the microarray technique. It is possible that the qRT-PCR approach provides a better sensitivity and resolution for molecular classification, which should be recommended for gene expression-based diagnosis.

The results described in this study may provide a strategy for classification of patients and potential therapy of metastatic HCC by converting the unique MIM to a MAM profile. Current pro-inflammatory-based postoperative therapies to prevent HCC recurrence show a beneficial effect; however, not all patients are sensitive to this treatment regimen. We speculate that postsurgical treatment with IFNG or perhaps other Th1-related cytokines in the MIM group may ameliorate the metastatic-related imbalance of cytokines toward that of nonmetastatic HCC patients. These adjuvant therapies may improve responses by selecting only the MIM group identified by the 17 gene predictor as those eligible and most likely to benefit from pro-inflammatory cytokine treatment. Thus, a confident determination of individual HCC patients who have either a MIM profile or a MAM may allow us to classify these patients in advance and thus provide ample time to select the most suitable treatments. This possibility remains to be determined and could significantly affect the clinical outcome of patients likely to develop HCC venous metastases.

Experimental procedures

Clinical specimens

Gene expression profiles were conducted in noncancerous hepatic fresh frozen tissues from 115 Asian HCC patients. Among them, 88% were male, 91% had underlying cirrhosis, and 96% were serologically positive for HBV (Table S1). Fifty-one percent of patients had a serum α-fetoprotein (AFP) level $\geq$ 300 ng/ml. The average age of this cohort was 50 years. These samples were categorized into two groups: 52 MIM and 63 MAM (see Supplemental Data). MIM (*m*etastasis-*i*nclined *m*icroenvironment) refers to hepatic tissues from patients with primary HCC lesions accompanied by venous metastases found in the portal vein, inferior vena cava, or common bile duct, or with solitary HCC subsequently having developed distant metastases that were confirmed at follow-up; MAM (*m*etastasis-*a*verse *m*icroenvironment) refers to hepatic tissues from patients carrying a single HCC lesion with no detectable metastases at the time of diagnosis and at follow-up. Of the 115 samples, 9 MIM and 11 MAM samples, which were used in our previous microarray study of HCC tumors, were chosen for the current microarray study so that a side-by-side comparison of the prognostic signatures from the tumors and noncancerous regions could be done. Hepatic tissue samples of 22 chronic liver disease noncancer patients with cirrhosis (AIH, autoimmune hepatitis [n = 6]; PBC, primary biliary cirrhosis [n = 8]; or HBV, hepatitis B virus [n = 8]) were also used in this study. In addition, eight normal liver tissues from disease-free patients who were liver donors without any detectable HCC or underlying liver conditions such as cirrhosis or dysplasia were used as a reference control in both microarray and qRT-PCR-based profiling. Total RNA from 54 hepatic tissue samples (8 normal liver, 22 chronic liver diseases, as well as 24 HCC patients [12 MIM and 12 MAM]) were from our previous studies (Kim et al., 2004; Ye et al., 2003). Total RNA from the additional 91 HCC hepatic tissues (40 MIM and 51 MAM) were obtained with informed consent from patients who underwent curative resection at the Liver Cancer Institute and Zhongshan Hospital (Fudan University, Shanghai, China). The study was approved by the Institutional Review Board of the Liver Cancer Institute and NIH. Immunohistochemical analysis of NOS2 was conducted on 68 independent paraffin-embedded hepatic tissues (37 MIM and 31 MAM) from HCC patients obtained from Zhongshan Hospital that were not used for gene expression profiling studies, except for five MIM and seven MAM.

cDNA microarrays, RNA isolation, and qRT-PCR

The cDNA microarray platform, RNA isolation, and microarray methodology were essentially as previously described (Ye et al., 2003). The microarray

data have been submitted to the Gene Expression Omnibus (GEO) public database at NCBI, and the accession number is GSE5093 (GSM114909-GSM114928). For qRT-PCR, isolated RNA was converted to cDNA using the High Capacity cDNA Archive Kit (Applied Biosystems, Foster City, CA). Reactions were performed with the ABI PRISM 7700 Sequence Detector System (Applied Biosystems) (see Supplemental Data). Human 18S RNA labeled with VIC reporter dye was used as an endogenous control. The cytokine expression profiles were quantified by qRT-PCR using the Taqman Cytokine Gene Expression Plate (Applied Biosystems) (see Supplemental Data). The reproducibility of the 17 gene signature assay was determined in triplicate on three separate plates with normal liver samples, and the standard deviations for these genes were 0.021 to 0.778.

Statistical analyses

Unsupervised hierarchical clustering analysis was performed by the GENESIS software version 1.5 developed by Alexander Sturn (IBMT-TUG, Graz, Austria). The BRB ArrayTools software V3.2.2 was also used for supervised and unsupervised analyses, as described previously (Ye et al., 2003). In the qRT-PCR-based profiling for class prediction utilizing the 17 gene signature, we used PAM (*p*rediction *a*nalysis of *m*icroarrays) developed by Tibshirani et al. (2002). Multidimensional scaling analysis based on Euclidean distance was used to visualize the classification outcome of the training and independent test cases. The Kaplan-Meier survival analysis was used to compare patient survival based on prediction results, using Excel-based WinSTAT software (http://www.winstat.com/). The statistical p value was generated by the Cox-Mantel log-rank test. Cox proportional hazards regression (univariate and multivariate tests) was used to analyze the effect of fifteen clinical variables on patient survival or recurrence using STATA 8.0 (College Station, TX) (see Supplemental Data). The statistical significance was defined as $p < 0.05$.

Immunohistochemistry, ELISA, and PBMC isolation

Immunohistochemical (IHC) staining was performed on 5 μm sections of paraffin-embedded tissue samples. Anti-NOS2 (BD Transduction Labs, San Diego, CA), anti-CSF1 (Santa Cruz Biotechnology, Inc., Santa Cruz, CA), anti-CD45 (BD Pharmingen, San Diego, CA), anti-DR (DakoCytomation, Carpinteria, CA), anti-CD68 (AbCAM, Cambridge, MA) were used to detect NOS2, CSF1, CD45, HLA-DR, and CD68, respectively. Detailed IHC protocols and quantification methods are described in the Supplemental Data. The CSF1 ELISA assay was performed on HCC and non-HCC serum samples (HBsAg carriers) using the M-CSF Quantikine Kit (R&D Systems, Inc., Minneapolis, MN). PBMC was isolated from healthy blood donor buffy coat (approved and provided by the NIH Department of Transfusion Medicine) by density-based centrifugation through histopaque (Sigma, St. Louis, MO). qRT-PCR on the cytokine plate was conducted as described above.

FACS analysis

Immunophenotypic analysis was performed by FACS using FITC-conjugated monoclonal antibody to CD3 (BD Pharmingen, San Diego, CA) and APC-conjugated monoclonal antibodies to IFNG or IL4. Freshly isolated human PBMCs (2×10^6 cells) were stained using the Cytofix/Cytoperm kit (BD Pharmingen, San Diego, CA) according to the manufacturer's protocol (see Supplemental Data). Cells were acquired by a FACsCalibur (BD Biosciences, San Diego, CA) using Cell Quest Pro software, and data analysis was performed using FlowJo software (Version 5.7.2, Tree Star, Inc.).

Supplemental data

The Supplemental Data include Supplemental Experimental Procedures, four supplemental figures, and six supplemental tables and can be found with this article online at http://www.cancercell.org/cgi/content/full/10/2/99/DC1/.

Acknowledgments

We thank Drs. J. Ashwell, W. Telford, J. Ortaldo, L. Jirmanova, and C.C. Harris for their invaluable comments and technical expertise; Ms. K. Meyer for GEO submission; and Ms. K. MacPherson for her bibliographic assistance. This work was supported by the Intramural Research Program of the Center for Cancer Research, the US National Cancer Institute. Q.-H.Y., H.-L.J, L.-X.Q., and Z.-Y.T. were also supported by research grants from the China National Natural Science Foundation for Distinguished Young Scholars (30325041), the China National "863" R&D High-Tech Key Project (2002BA711A02-4), the State Key Basic Research Program of China (N. G1998051210), and the Key Program Project of National Natural Science Foundation of China (30430720).

Received: March 10, 2006
Revised: May 12, 2006
Accepted: June 27, 2006
Published: August 14, 2006

References

Ambs, S., Merriam, W.G., Ogunfusika, M.O., Bennett, W.P., Ishibe, N., Hussain, S.P., Tzeng, E.E., Geller, D.A., Billiar, T.R., and Harris, C.C. (1998). p53 and vascular endothelial growth factor regulate tumour growth of NOS2-expressing human carcinoma cells. Nat. Med. *4*, 1371–1376.

Berghella, A.M., Contasta, I., Pellegrini, P., Del Beato, T., and Adorno, D. (2002). Peripheral blood immunological parameters for use as markers of pre-invasive to invasive colorectal cancer. Cancer Biother. Radiopharm. *17*, 43–50.

Bernards, R., and Weinberg, R.A. (2002). A progression puzzle. Nature *418*, 823.

Coussens, L.M., and Werb, Z. (2002). Inflammation and cancer. Nature *420*, 860–867.

D'Arrigo, A., Belluco, C., Ambrosi, A., Digito, M., Esposito, G., Bertola, A., Fabris, M., Nofrate, V., Mammano, E., Leon, A., et al. (2005). Metastatic transcriptional pattern revealed by gene expression profiling in primary colorectal carcinoma. Int. J. Cancer *115*, 256–262.

Dave, S.S., Wright, G., Tan, B., Rosenwald, A., Gascoyne, R.D., Chan, W.C., Fisher, R.I., Braziel, R.M., Rimsza, L.M., Grogan, T.M., et al. (2004). Prediction of survival in follicular lymphoma based on molecular features of tumor-infiltrating immune cells. N. Engl. J. Med. *351*, 2159–2169.

de Visser, K.E., and Coussens, L.M. (2005). The interplay between innate and adaptive immunity regulates cancer development. Cancer Immunol. Immunother. *54*, 1143–1152.

Fidler, I.J. (1995). Modulation of the organ microenvironment for treatment of cancer metastasis. J. Natl. Cancer Inst. *87*, 1588–1592.

Fidler, I.J., and Kripke, M.L. (2003). Genomic analysis of primary tumors does not address the prevalence of metastatic cells in the population. Nat. Genet. *34*, 23.

Golden-Mason, L., and Rosen, H.R. (2006). Natural killer cells: Primary target for hepatitis C virus immune evasion strategies? Liver Transpl. *12*, 363–372.

Hanahan, D., and Weinberg, R.A. (2000). The hallmarks of cancer. Cell *100*, 57–70.

Hattori, E., Okumoto, K., Adachi, T., Takeda, T., Ito, J., Sugahara, K., Watanabe, H., Saito, K., Saito, T., Togashi, H., and Kawata, S. (2003). Possible contribution of circulating interleukin-10 (IL-10) to anti-tumor immunity and prognosis in patients with unresectable hepatocellular carcinoma. Hepatol. Res. *27*, 309–314.

Hofseth, L.J., Saito, S., Hussain, S.P., Espey, M.G., Miranda, K.M., Araki, Y., Jhappan, C., Higashimoto, Y., He, P., Linke, S.P., et al. (2003). Nitric oxide-induced cellular stress and p53 activation in chronic inflammation. Proc. Natl. Acad. Sci. USA *100*, 143–148.

Hunter, K.W. (2004). Host genetics and tumour metastasis. Br. J. Cancer *90*, 752–755.

Hunter, K.W., and Crawford, N.P. (2006). Germ line polymorphism in metastatic progression. Cancer Res. *66*, 1251–1254.

Hussain, S.P., Hofseth, L.J., and Harris, C.C. (2003). Radical causes of cancer. Nat. Rev. Cancer *3*, 276–285.

Iizuka, N., Oka, M., Yamada-Okabe, H., Nishida, M., Maeda, Y., Mori, N., Takao, T., Tamesa, T., Tangoku, A., Tabuchi, H., et al. (2003). Oligonucleotide

microarray for prediction of early intrahepatic recurrence of hepatocellular carcinoma after curative resection. Lancet *361*, 923–929.

Johansson, S., Hall, H., Berg, L., and Hoglund, P. (2006). NK cells in autoimmune disease. Curr. Top. Microbiol. Immunol. *298*, 259–277.

Johnson, T.R., Hong, S., Van Kaer, L., Koezuka, Y., and Graham, B.S. (2002). NK T cells contribute to expansion of CD8(+) T cells and amplification of antiviral immune responses to respiratory syncytial virus. J. Virol. *76*, 4294–4303.

Kim, J.W., Ye, Q., Forgues, M., Chen, Y., Budhu, A., Sime, J., Hofseth, L.J., Kaul, R., and Wang, X.W. (2004). Cancer-associated molecular signature in the tissue samples of patients with cirrhosis. Hepatology *39*, 518–527.

Lee, J.S., Chu, I.S., Heo, J., Calvisi, D.F., Sun, Z., Roskams, T., Durnez, A., Demetris, A.J., and Thorgeirsson, S.S. (2004). Classification and prediction of survival in hepatocellular carcinoma by gene expression profiling. Hepatology *40*, 667–676.

Liotta, L.A. (1985). Mechanisms of cancer invasion and metastasis. Important Adv. Oncol. 28–41.

Mann, J.R., Backlund, M.G., and DuBois, R.N. (2005). Mechanisms of disease: Inflammatory mediators and cancer prevention. Nat. Clin. Pract. Oncol. *2*, 202–210.

Mantovani, A., Sozzani, S., Locati, M., Allavena, P., and Sica, A. (2002). Macrophage polarization: tumor-associated macrophages as a paradigm for polarized M2 mononuclear phagocytes. Trends Immunol. *23*, 549–555.

Mueller, M.M., and Fusenig, N.E. (2004). Friends or foes—bipolar effects of the tumour stroma in cancer. Nat. Rev. Cancer *4*, 839–849.

Nakakura, E.K., and Choti, M.A. (2000). Management of hepatocellular carcinoma. Oncology (Huntingt.) *14*, 1085–1098.

Paludan, S.R., Malmgaard, L., Ellermann-Eriksen, S., Bosca, L., and Mogensen, S.C. (2001). Interferon (IFN)-gamma and Herpes simplex virus/tumor necrosis factor-alpha synergistically induce nitric oxide synthase 2 in macrophages through cooperative action of nuclear factor-kappa B and IFN regulatory factor-1. Eur. Cytokine Netw. *12*, 297–308.

Pixley, F.J., and Stanley, E.R. (2004). CSF-1 regulation of the wandering macrophage: complexity in action. Trends Cell Biol. *14*, 628–638.

Pollard, J.W. (2004). Tumour-educated macrophages promote tumour progression and metastasis. Nat. Rev. Cancer *4*, 71–78.

Ramaswamy, S., Ross, K.N., Lander, E.S., and Golub, T.R. (2003). A molecular signature of metastasis in primary solid tumors. Nat. Genet. *33*, 49–54.

Smyth, M.J., Cretney, E., Kershaw, M.H., and Hayakawa, Y. (2004). Cytokines in cancer immunity and immunotherapy. Immunol. Rev. *202*, 275–293.

Spirli, C., Fabris, L., Duner, E., Fiorotto, R., Ballardini, G., Roskams, T., LaRusso, N.F., Sonzogni, A., Okolicsanyi, L., and Strazzabosco, M. (2003). Cytokine-stimulated nitric oxide production inhibits adenylyl cyclase and cAMP-dependent secretion in cholangiocytes. Gastroenterology *124*, 737–753.

Tang, Z.Y. (2001). Hepatocellular carcinoma—Cause, treatment and metastasis. World J. Gastroenterol. *7*, 445–454.

Thorgeirsson, S.S., and Grisham, J.W. (2002). Molecular pathogenesis of human hepatocellular carcinoma. Nat. Genet. *31*, 339–346.

Tibshirani, R., Hastie, T., Narasimhan, B., and Chu, G. (2002). Diagnosis of multiple cancer types by shrunken centroids of gene expression. Proc. Natl. Acad. Sci. USA *99*, 6567–6572.

van de Vijver, M.J., He, Y.D., van't Veer, L.J., Dai, H., Hart, A.A., Voskuil, D.W., Schreiber, G.J., Peterse, J.L., Roberts, C., Marton, M.J., et al. (2002). A gene-expression signature as a predictor of survival in breast cancer. N. Engl. J. Med. *347*, 1999–2009.

Van Dommelen, S.L., and Degli-Esposti, M.A. (2004). NKT cells and viral immunity. Immunol. Cell Biol. *82*, 332–341.

Ye, Q.H., Qin, L.X., Forgues, M., He, P., Kim, J.W., Peng, A.C., Simon, R., Li, Y., Robles, A.I., Chen, Y., et al. (2003). Predicting hepatitis B virus-positive metastatic hepatocellular carcinomas using gene expression profiling and supervised machine learning. Nat. Med. *9*, 416–423.

Yuki, K., Hirohashi, S., Sakamoto, M., Kanai, T., and Shimosato, Y. (1990). Growth and spread of hepatocellular carcinoma. A review of 240 consecutive autopsy cases. Cancer *66*, 2174–2179.

Zingoni, A., Sornasse, T., Cocks, B.G., Tanaka, Y., Santoni, A., and Lanier, L.L. (2005). NK cell regulation of T cell-mediated responses. Mol. Immunol. *42*, 451–454.

Accession numbers

The microarray data have been submitted to the Gene Expression Omnibus (GEO) public database at NCBI, and the accession number is GSE5093 (GSM114909-GSM114928).